Polypyrrole-Graphene Quantum dots Nanocomposite Layer for Detection of Uric Acid Using Plasmonic Sensor

A.R Sadrolhosseini [a], and S. M. Hamidi[a]

[a] Magneto-plasmonic Lab, Laser and Plasma Research Institute, Shahid Beheshti University, Tehran, Iran
*** Corresponding author email: m_hamidi@sbu.ac.ir**

Received: Dec. 18, 2021, Revised: Mar. 4, 2022, Accepted: Mar. 12, 2022, Available Online: Mar. 12, 2022
DOI: 10.30495/ijbbo.2021.689782

ABSTRACT— A polypyrrole-graphene quantum dots nanocomposite layer was prepared on the surface of the gold layer for detection of the uric acid using the surface plasmon resonance technique. The X-ray diffraction spectrum and the field emission scanning electron microscopy image for polypyrrole-graphene quantum dots layer confirmed the graphene quantum dots scattered on the surface of the polymer and the nanocomposite layer formed on the surface of thin gold layer in the thickness of 45.3 nm. The minimum concentration of uric acid that was detected by the sensing layer was about 1 ppm and the affinity constant of polypyrrole-graphene quantum dots for detection of uric acid was larger than the affinity constant for detection of ascorbic acid and glucose. The response of the polypyrrole-graphene quantum dots is larger than the response of polypyrrole for the detection of uric acid.

KEYWORDS: Surface plasmon resonance, polypyrrole-graphene quantum dots, uric acid, glucose, ascorbic acid.

I. INTRODUCTION

The surface plasmon resonance (SPR) sensor is a versatile technique to detect and measure the low concentration of toxic chemicals and biomaterial. Uric acid, glucose, cholesterol, triglyceride, and creatinine are the common blood biochemistry components and they must be measured to control the blood chemistry. Among these blood chemistry components, uric acid is a significant biomolecule because uric acid involves in the production of the metabolism of purines [1] and it is the ultimate catabolite of purine metabolism in humans and the backbone of Desoxyribonucleic acid (DNA) [2]. Uric acid is an organic acid with a pH of about 5.5. Uric acid is a heterocyclic carbon with the chemical formula $C_5H_4N_4O_3$. The level of uric acid is one of the significant parameters to diagnose and detect illnesses such as gout. Moreover, uric acid has important role in the universal food chain for plant because it is a source of nitrogen, carbon and oxygen [2]. The uric acid is oxidized by the electrode; hence, the level of uric acid can be measured using electro-chemistry [3, 4] and colorimetric [1] methods.

The spectroscopy methods such as SPR and fluorescence [5] techniques were used to measure the amount of uric acid in human fluids and environmental solutions. For example, the SPR sensor based on wavelength modulation was used to measure the uric acid using MoS_2-graphene nanocomposite [6]. The uricase entrapped polyacrylamide gel was employed to detect the uric acid using fiber optics SPR sensor [7]. The accuracy for detection of uric acid was about 0.9mM. Therefore, the SPR sensor has the potential to measure and detect uric acid.

The SPR depends on the optical properties of metal and dielectric layers, and it is related to charge density oscillation at the interface of a metal and dielectric medium. Hence, the gold or silver layers have the main role to generate the SPR signals in the SPR sensors, and the sensing

layers based on the nanostructures [8] are used to enhance the sensitivity and selectivity of the SPR sensors. Graphene, MoS_2, gold [9], silver [10], and ZnO nanoparticles [11] are the common nanostructures for improving the sensing layer. In this study, the polypyrrole-graphene quantum dots (PPy-GQD) nanocomposite layer was prepared on the surface of the gold layer for the detection of uric acid. The prepared layer was characterized using analytical methods.

II. Materials and Methods

A. *Materials*

Pure sodium dodecylbenzensulfonate (SDBS), graphene quantum dots, and pyrrole (Py) have been purchased from Sigma-Aldrich Company. Uric acid, ascorbic acid, and glucose were purchased from PubChem Company in the commercial grid.

B. *Preparation of PPy Layer and PPy-GQD Layer*

The preparation of PPy and PPy-GQD layers were presented in the Ref. [12, 13]. The gold (45.3 nm), PPy and PPy-GQD layers were coated on the surface of a thin glass slide using the sputtering coating and electrodeposition techniques (Auto-lab PGSTAT 101), respectively. The PPy-GQD was deposited on the surface of a gold-coated glass slide via electrochemical polymerization of pure and distilled pyrrole in the presence of graphene quantum dots. The ratio of graphene quantum dots and the sodium dodecylbenzensulfonate (SDBS) was about 1:3 and the mixture were sonicated for 3 hours. The monomer solution included 0.1 M pyrrole, 100 ppm graphene quantum dots, and SDBS. The polymerization of pyrrole was carried out at the constant potential of 0.83 V. The reference electrode, working electrode, and counter electrode were saturated calomel electrodes (SCE), graphite electrodes, and gold-coated glass slide, respectively and the electrodeposition time was 11 seconds. The prepared layer was tested using X-ray diffraction spectroscopy (XRD), field emission electron microscopy (FE-SEM), and a profile meter (AMBIOS, XP-200).

The PPy sensing layer was deposited on a surface of the gold layer. The PPy layer was electrochemically prepared in a solution containing 0.3 M Pyrrole (pre-distilled), 0.1 M p-toluene sulfonate (P-TS) dopant at room temperature for 11 seconds.

C. *Preparation of Analyte*

To prepare the solution of uric acid in the different concentrations, 1 g of uric acid powder was dissolved in 1 L of deionized distilled water at room temperature. The solution was sonicated for 1 h to obtain the homogeneous solution. The prepared solution contained 1000 ppm of uric acid. Subsequently, the low concentrations of the uric acid solution, being 1, 3, 5, 10, 25, and 50 ppm were separately prepared by the systematic dilution of 1000 ppm of prepared solution in deionized distilled water. This method was separately used to prepare the ascorbic acid and glucose at the concentration of 1, 3, 5, 10, 25, and 50 ppm.

D. *SPR Setup*

The SPR setup contains a high index prism (ZF 52, n = 1.83956, A = 60°, Foctek) a He-Ne laser (632.8 nm) a polarizer, a pinhole, a chopper, a precision rotation stage, and lock-in amplifier. The gold coated glass slide was attached to the high index prism using a liquid index match. The prism was rotated up to 30º.

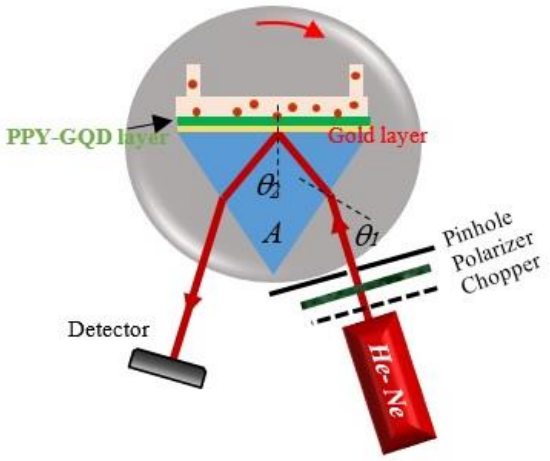

Fig. 1 The SPR setup contains a high index prism, a He-Ne laser, a detector, a chopper, a polarizer, a pinhole, and a rotation stage.

The detector was registered the laser intensity when the rotation stage momentarily stopped

and the SPR signal was achieved. The SPR signal is a function of the refractive index, the thickness of layers, and the refractive index of an analyte. The SPR signals were analyzed based on Fresnel's theory to find the resonance angle [12, 14].

The reflectance is a function of the wavelengths, refractive indices of the gold, sensing layer, and analyte alongside the thicknesses of the gold and sensing layers. In this experiment, the thickness and the refractive index of the gold layer were 45.3 nm, and 0.235+3.31i, respectively. The optical parameter of the sensing layer can be obtained by minimizing the summation of the theoretical (R_{Th}) and the experimental (R_{Ex}) values of the reflectance. The equation is then as follows [15]:

$$\Omega = \sum_{\theta} [R_{Th}(\theta, n) - R_{Ex}(\theta, n)] \quad (1)$$

III. Results and Discussion

Figure 2(a) shows the XRD spectra for pure GQD, pure PPy and PPy-GQD composite layer. The main peaks appeared at 21.3º and 25.1º and the sharp and broad peaks overlapped at centered 25° together, that confirms the GQD formed in the PPy layer [15-18]. Figures 2(b) and 2(c) show the morphology of PPy-GQD and PPy as sensing layers. The polymer layers (PPy and PPy-GQD) formed on the surface of the substrate and it can find, the GQD is scattered at the surface of the polymer as a comparison of Fig 2(b) and 2(c).

The PPy-GQD and PPy layers were separately attached to the surface of the high index prism and the distilled water has flowed on the tank. The SPR signals were registered to find the refractive index of PPy-GQD, PPy composite layers and the baseline. Figure 3 shows the SPR signals and they were analyzed using Fresnel's equation. The solid lines were fitted to the experimental values (dotted point) and the resonance angles and the refractive indies of PPy-GQD and PPy layers were achieved at 55.58º, 55.832º (baseline) and 1.6709+0.118i, 1.6731+0.145i, respectively.

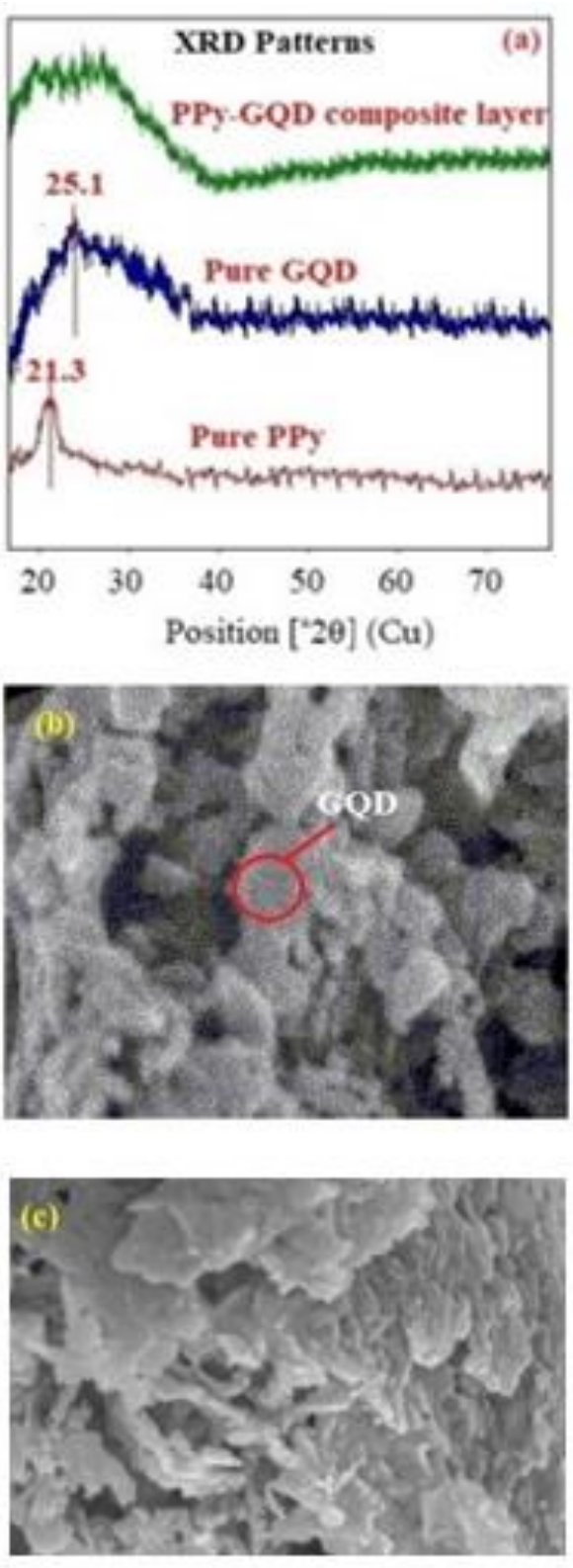

Fig. **2** a) The XRD pattern for pure PPy, pure GQD and PPy-GQD layer; b) FE-SEM image for PPy-GQD layer; and c) FE-SEM image for PPy layer

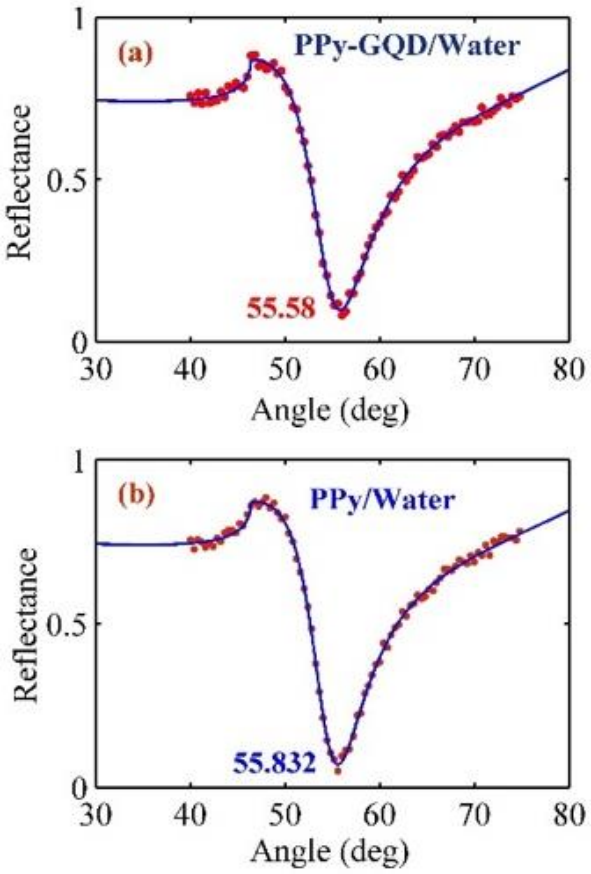

Fig. **3** The SPR signals a) PPy-GQD layer and b) PPy layer at the baseline were 55.58º, and 55.832º, respectively. The thickness and refractive index of the gold layer were 45.3 nm and 0.235+3.31i, respectively. The thickness of PPy-GQD and PPy layers was measured using the profilometer and they 13.3 ± 0.5 nm and 14± 0.5 nm.

The uric acid was flowed separately in the different concentrations in the sample tank and the SPR signals (Fig. 4) were registered. The SPR signals were analyzed using Fresnel's equation. The resonance angle was in the range of 55.643º to 55.798º. The experiment was repeated for ascorbic acid and glucose separately and Figure 5, 6 depict the SPR signals at the equilibrium value. As a result, the resonance angle for detection of ascorbic acid and glucose changed in the range of 55.623º to 55.717º and 55.616º to 55.701º, respectively. The variation of resonance angle with the concentration of uric acid were calculated from baseline.

Figure 7 depicts the angle shifts versus the concentrations of uric acid, ascorbic acid, and glucose. Variation of the resonance angle is a function of concentration and it fit Langmuir's formula as follows [19]:

$$\Delta\theta = \frac{(\Delta\theta_{\max} \times C)}{\frac{1}{K_b} + C} \qquad (2)$$

where $\Delta\theta_{\max}$, K_b , and C are the resonance angle shift at the maximum value, the equilibrium constant, and the concentration of analyte, respectively.

The equilibrium constant is inversely related to the affinity of the sensing layer (PPy-GQD composite layer) for capping the analyte [19]. The affinity constant of PPy-GQD layer for bonding the uric acid, ascorbic acid, and glucose are 4.2680, 3.6819, and 3.3807, respectively. As a result, the PPy-GQD composite layer has a greater tendency to cap the uric acid than the ascorbic acid and glucose. The sensitivity of the sensor ($\Delta(\Delta\theta)/\Delta C$) has been calculated from the slope of the plot in Fig. 5. The $\Delta\theta_{max}$ for uric acid, ascorbic acid, and glucose are 0.2358, 0.1457, and 0.129, respectively. Hence, the sensitivity for detection of uric acid, ascorbic acid, and glucose was achieved at 0.0049, 0.0029, and 0.0024 deg/ppm, respectively. Therefore, the sensitivity of the sensor for the detection of uric acid is larger than the sensitivity of the sensor for the detection of ascorbic acid and glucose.

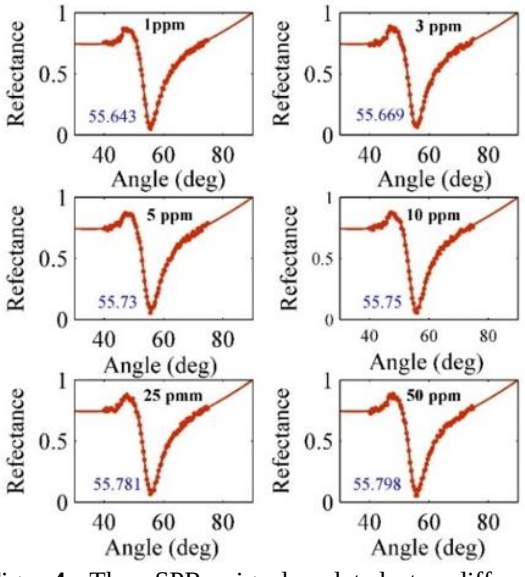

Fig. **4** The SPR signal related to different concentrations of uric acid at the saturation value.

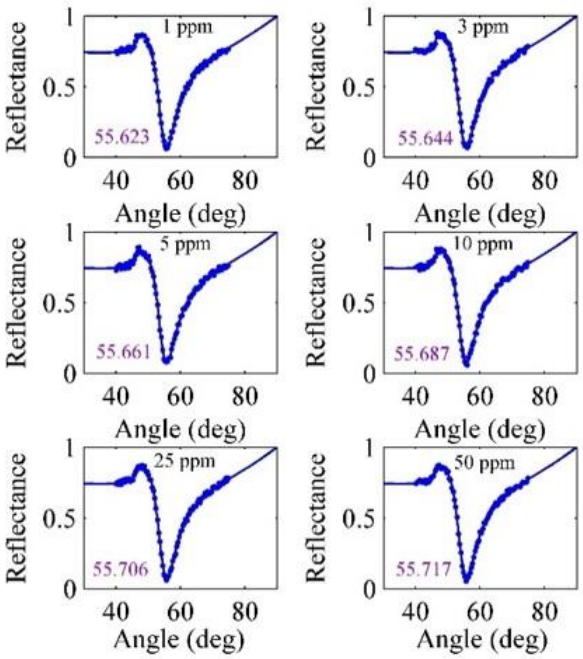

Fig. **5** The SPR signals for detection of ascorbic acid at the saturation value.

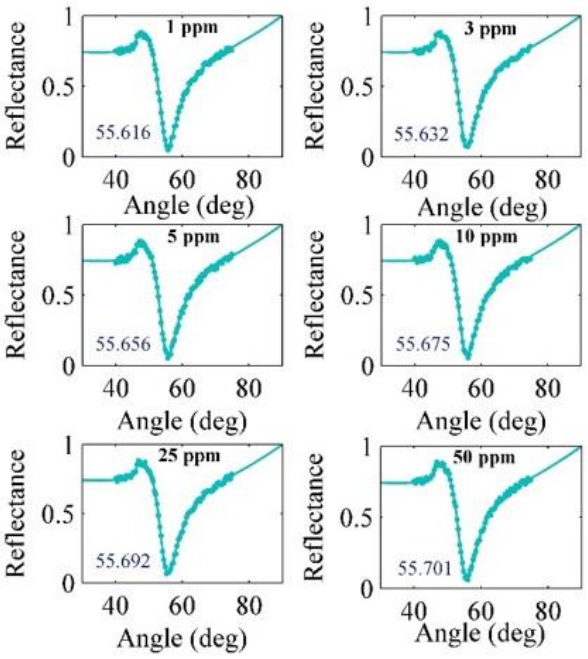

Fig. **6** The SPR signals for detection of glucose at the saturation value.

Figure 8 shows the SPR signals related to PPy layer for the detection of uric acid and the resonance angle is in the range of 55.884º to 55.981º.

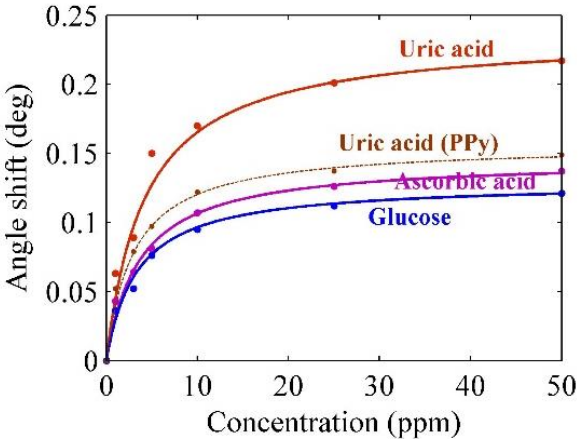

Fig. **7** Variation of resonance angle shift with different concentrations of uric acid, ascorbic acid, and glucose when the PPy-GQD was used as a sensing layer. The equilibrium constant for uric acid, ascorbic acid, and glucose are 0.2343, 0.2716, and 0.2958, respectively. The variation of resonance angle shift was experimentally achieved when the uric acid was contacted with the PPy layer.

The variation of resonance angle with different concentrations of uric acid when the uric acid interacted with the PPy layer, was presented in the Fig 7. As an experimental result, the maximum angle shift occurred at 0.157. The equilibrium, affinity constants, and sensitivity are 0.3332, 3.0012, and 0.0028 deg/ppm respectively. Consequently, the sensitivity of PPy-GQD is larger than the sensitivity of PPy layer for the detection of uric acid. So, the GQD enhanced the tendency of the sensing layer to detect uric acid

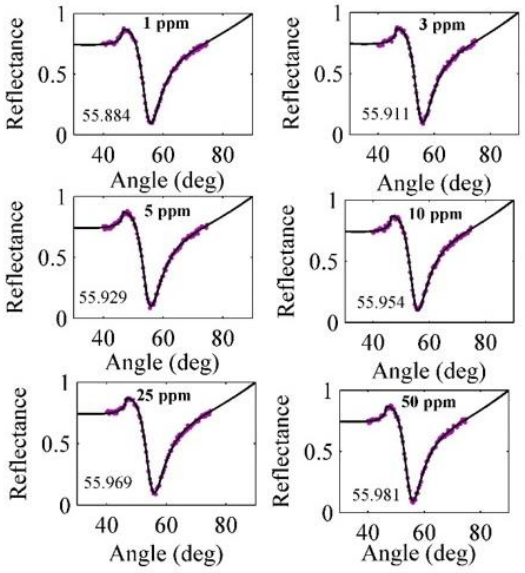

Fig. **8** The SPR signals for detection of uric acid in the presence of PPy layer at the saturation value.

The polypyrrole capped the graphene quantum dots during the elector-polymerization of pyrrole. GQD attached to PPy at the edge of the molecules, as that was where electrons were made available to the polymer. Furthermore, the uric acid interacted with the carboxylic group of GQD, which was an agent between uric acid and PPy. Hence, the resonance angle increased when the analyte interacts with the sensing layer. Consequently, the PPy-GQD layer is capable of adsorbing uric acid.

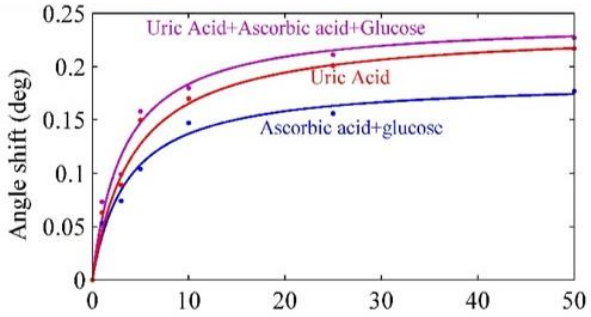

Fig.**9** The variation of resonance angle shift for mixture of uric acid, ascorbic acid and glucose in the presence of PPy-GQD

In order to test the selectivity of the PPy-GQD sensing layer, the mixture of ascorbic acid with glucose and the mixture of uric acid with ascorbic acid and glucose were contacted to the sensing layer. The variation of angle shift with the different concentration of the mixture (Figure 9) shows the response of sensing layer in the presence of uric acid is larger than the response of sensing layer in other case. Consequently, the sensor can detect the uric acid better than glucose and ascorbic acid.

IV. CONCLUSION

The PPy-GQD was deposited on the surface of the gold thin layer using the electrodeposition technique. The analytical methods confirmed that the GQD formed and scattered on the surface of PPy during electro-polymerization of pyrrole. The thickness and the refractive of the PPy-GQD layer were 13.3 nm and 1.6709+0.118i, respectively. The resonance angle shift was separately obtained in the presence of uric acid, ascorbic acid, and glucose. As a result, the variation of resonance angle for uric acid was larger than the resonance angle shift for ascorbic acid and glucose. The detection of uric acid was tested with PPy layer. The result confirmed the sensitivity of PPy-GQD nanocomposite sensing layer is larger than PPy sensing layer. Consequently, the affinity constant of the PPy-GQD nanocomposite layer for the detection of uric acid was larger than the affinity constant of the sensing layer for the detection of ascorbic acid and glucose. Hence, PPy-GQD nanocomposite layer is a suitable sensing layer for the detection of uric acid

REFERENCES

[1] H. K. Walker, W. D. Hall and J. W. Hurst, *Clinical Methods: The History, Physical, and Laboratory Examinations*, in Uric Acid 3rd Ed. Boston, Butterworths,1990.

[2] R. Barsoum and M. El-Khatib, "Uric acid and life on earth," J Adv Res. Vol. 8, pp.471–474, 2017.

[3] J. Guo, "Uric Acid Monitoring with a Smartphone as the Electrochemical Analyzer," Anal. Chem. Vol. 88, pp.11986–11989, 2016.

[4] Q. Yan, N. Zhi, L. Yang, G. Xu, Q. Feng, Q. Zhang, and S. Sun, "A highly sensitive uric acid electrochemical biosensor based on a nano-cube cuprous oxide/ferrocene/uricase modified glassy carbon electrode," Sci. Rep. vol.10, pp. 10607, 2020.

[5] J. Yang, Z. Huang, Y. Hu, J. Ge, J. Li, and Z. Li, "A facile fluorescence assay for rapid and sensitive detection of uric acid based on carbon dots and MnO2 nanosheets," New J. Chem. Vol. 42. pp.15121-15126, 2018.

[6] N. A. Jamil, G. S. Mei, N. B. Khairulazdan, S. P. Thiagarajah, A. A. Hamzah, and B. Y. Majlis, "Detection of Uric Acid Using Kretschmann-based SPR Biosensor with MoS2-Graphene," IEEE Xplore, pp.18671720 (1-4), 2019.

[7] R. Kant, R. Tabassum, and B. D Gupta, "Fiber optic SPR-based uric acid biosensor using uricase entrapped polyacrylamide gel," IEEE Photon. Technol. Lett. Vol. 28, pp. 2050 - 2053, 2016.

[8] P.Kannan and S. A. John, "Determination of nanomolar uric and ascorbic acids using enlarged gold nanoparticles modified

electrode," Anal Biochem. Vol. 386, pp. 65-72, 2009.

[9] N. Stozhko, M. Bukharinova, L. Galperin, and K. Brainina, "A Nanostructured Sensor Based on Gold Nanoparticles and Nafion for Determination of Uric Acid," Biosensors (Basel). vol 6, pp.1-13, 2018.

[10] Q. Dai, T. Wei, C. Lv, and F. Chai, "Facile preparation of Ag nanoparticles using uric acid and their applications in colorimetric detection and catalysis," Anal. Methods. vol. 10. pp. 4518-4524, 2018.

[11] Y. Wang, L. Yu, Z. Zhu, J. Zhang, and J. Zhu. "Novel Uric Acid Sensor Based on Enzyme Electrode Modified by ZnO Nanoparticles and Multiwall Carbon Nanotubes," Anal. Lett. Vol. 42, pp. 775-789, 2009.

[12] A. R. Sadrolhosseini, A. S. M. Noor, A. Bahrami, H.N. Lim, Z. A. Talib, and M. A. Mahdi, "Application of Polypyrrole Multi-walled Carbon Nanotube Composite Layer for Detection of Mercury, Lead and Iron Ions Using Surface Plasmon Resonance Technique," PlosOne. Vol. 9, e93962 (1-10), 2014.

[13] A. R. Sadrolhosseini, S. Shafie, S. A. Rashid, and M. A. Mahdi, "Surface plasmon resonance measurement of arsenic in low concentration using polypyrrole-graphene quantum dots layer," Measurement. Vol. 173, pp. 108546 (1-4), 2019.

[14] A. R. Sadrolhosseini, A. S. M. Noor, and M. M. Moksin, *Application of Surface Plasmon Resonance Based on a Metal Nanoparticle in Plasmonics - Principles and Applications*, K. Y. Kim, Ed. London: IntechOpen, 2012.

[15] G. Ruhi, O.P. Modi and S. K. Dhawan, "Chitosan-polypyrrole-SiO_2 composite coatings with advanced anticorrosive properties," Synth. Met. vol. 200. pp. 24-39, 2015.

[16] N. Hashemzadeh, M. Hasanzadeh, N. Shadjou, J. Eivazi-Ziaei, M. Khoubnasabjafari, and A. Jouyban, "Graphene quantum dot modified glassy carbon electrode for the determination of doxorubicin hydrochloride in human plasma," J. Pharm. Anal. Vol. 6, pp.235-241, 2016.

[17] S. Ramachandran, M. Sathishkumar, N. K. Kothurkar, and R. Senthilkumar, "Synthesis and characterization of graphene quantum dots/cobalt ferrite nanocomposite," IOP Conf. Series: Mater. Sci. Eng. Vol. 310, pp. 012139 (1-9), 2018.

[18] K. D. Kowanga, E. Gatebe, G. O. Mauti, and E. M. Mauti, "Kinetic, sorption isotherms, pseudo first-order model and pseudo-second-order model studies of Cu (II) and Pb(II) using defatted Moringa oleifera seed powder," J. Phytopharm, vol. 5, pp. 71-78, 2016.

[19] P. Moozarm Nia, W. P. Meng, and Y. Alias, "One-Step Electrodeposition of Polypyrrole-Copper Nano Particles for H_2O_2 Detection. J. Electrochem," Soc. Vol. 163, pp. B8-B14, 2016.

THIS PAGE IS INTENTIONALLY LEFT BLANK.